

Nucleation Enhancement Effect in Poly(L-lactide) (PLLA)/Poly(ϵ -caprolactone) (PCL) Blend Induced by Locally Activated Chain Mobility Resulting from Limited Miscibility

Fuji Sakai, Kenichi Nishikawa, Yoshio Inoue, and Koji Yazawa*

Department of Biomolecular Engineering, Tokyo Institute of Technology, 4259 Nagatsuta-cho, Midori-ku, Yokohama, Kanagawa 226-8501, Japan

Received July 16, 2009; Revised Manuscript Received October 1, 2009

ABSTRACT: The enhancement effect of nucleation in immiscible blend systems has recently attracted interest. Although several authors have reported that the effect occurs at the phase interface, little is known about the mechanism involved. We focused on poly(L-lactide) (PLLA)/poly(ϵ -caprolactone) (PCL) immiscible blend systems in which the presence of PCL enhanced the nucleation of PLLA at low temperature. We investigated the nucleation behavior of PLLA during aging at temperatures below T_g . Generally, neat polymers, including PLLA, seldom generate nuclei below T_g due to restrictions in chain mobility. However, through DSC analysis of the crystallization behavior following an aging process, we revealed that the nucleation of PLLA occurs during aging even at temperatures below T_g in the PLLA/PCL blend. Since the nuclei density became saturated with increasing aging time, the nucleation behavior was regarded as heterogeneous nucleation. The asymptotic density of nuclei depended on the PCL content, indicating that dispersed PCL acted as active sites for nucleation. The nucleation rate R was almost independent of the aging temperature, suggesting that the marked decrease in chain mobility due to the glass transition is locally evaded at the active sites. Nucleation was observed even at temperatures as much as 40 °C lower than T_g following the addition of only 1 wt % PCL, while the T_g obtained by a DSC heating scan showed a subtle decrease. This suggests that the limited miscibility of PLLA/PCL leads to the aggregation of PCL and induces local and deep depression of T_g at the interface of the PCL domains, resulting in marked enhancement of PLLA nucleation.

Introduction

Polymer blends have been investigated with a view to establishing simple and efficient methods to generate new high-performance materials. While some polymer mixtures are completely miscible at the molecular level, most blends are immiscible. One feature of immiscible polymer blends is the presence of separated domains and interfaces. The phase morphology and phase interface influence the mechanical properties of the bulk. For example, the impact resistance of immiscible blends is strongly related to the adhesive property of the phase interface.^{1,2} The adhesive ability is influenced by the interface structure such as the entanglement of polymer chains³ and crystal morphology.⁴ Therefore, information concerning the structure of the phase interface is crucial in efforts to control the mechanical function of polymeric materials. The preferential nucleation of crystals near the phase interface in immiscible polymer blends has recently attracted scientific interest.

Poly(L-lactide) (PLLA)/poly(ϵ -caprolactone) (PCL) is a typical immiscible blend of biocompatible polymers which has been extensively investigated in the context of formulating practical applications.^{5–11} Given the many biocompatible polyesters which tend to be inferior in mechanical strength to the universal polymers, the sufficient hardness of PLLA is expected to lend itself to industrial use. PCL is a much more flexible biocompatible polymer and is added to PLLA with the expectation of compensating for certain undesirable characteristics of PLLA such as brittleness and low flow rate for processing, without interfering with the original biocompatibility of PLLA.^{9,10} In previous

reports, the addition of PCL enhanced the cold crystallization of PLLA, while there was little effect on the melt crystallization.^{10,11} Since the effect is observed even with PCL content as low as 5 wt %, PCL seems to accelerate the generation of nuclei. However, the detailed mechanism involved remains to be determined.

The enhancement effect of nucleation in immiscible blends has been documented in several papers. In early reports, Bartczak et al. investigated the crystallization of isotactic polypropylene (iPP) in the presence of amorphous atactic polystyrene (aPS)¹² and reported preferential nucleation of iPP at the surface of the aPS phase by POM observations. The authors suggested that the enhancement effect is caused by a decrease in the surface free energy of formation of crystal nuclei due to presence of the phase interface. Wenig et al. investigated the crystallization kinetics of iPP/ethylene–propylene–diene terpolymer (EPDM) blends.¹³ The nuclei density of iPP increased by blending both crystalline and amorphous EPDMs. Avrami analysis of the isothermal crystallization revealed that the crystallization kinetics changed from a homogeneous nucleation system in neat iPP to a heterogeneous system in the iPP/EPDM blend, which indicates that the nucleation of iPP was enhanced heterogeneously at the surface of dispersed EPDMs domains. They also suggested that this resulted from a lowering of the surface free energy. In more recent reports, Tsuburaya et al. reported that nucleation occurred with liquid–liquid phase separation (LLPS) simultaneously in PS/poly(ethylene oxide) (PEO) blend systems.¹⁴ Han et al. also investigated the relation between nucleation and LLPS in the poly(ethylene-co-butene) (PEB)/poly(ethylene-co-hexene) (PEH) blend system and claimed that the nuclei mainly resided near the interface of the phases, as determined by AFM observations.^{15–17}

*Corresponding author. E-mail: kyazawa@bio.titech.ac.jp.

They speculated that the diffusion flux associated with the phase separation induced a specific orientation of polymer chains, thereby resulting in nucleation. Han et al. have also provided a computational simulation of nucleation in the polymer blend undergoing LLPS.¹⁸ Results indicated the generation of nuclei with high probability near the phase interface. As mentioned above, the phase interface seems to play a pivotal role in the nucleation enhancement effect in immiscible blends. However, the mechanism involved has not been sufficiently clarified. An understanding of the nucleation mechanism is important for controlling crystal morphology. Moreover, the delineation of the nucleation events is critical since these might influence the interface structure, which markedly influences the bulk property.

Experiments concerning nucleation in immiscible blends have been conducted at the optimum temperature for crystallization, which lies between the melting temperature (T_m) and glass transition temperature (T_g). At that temperature, since both nucleation and crystal growth occur competitively, the growth of the crystal hinders close observation of the nucleation behavior using methodologies based on calorimetry or microscopy. In the case of the PLLA/PCL blend, the cold crystallization is enhanced and suggests that the nucleation of PLLA is enhanced at lower temperature, probably even below T_g of PLLA. For neat PLLA, both the crystal growth and nucleation must freeze below T_g due to restrictions in chain mobility.^{19,20} However, since the nucleation is spacially a local phenomenon, it might occur at the interface of PCL domains. In the present study, therefore, we focused on nucleation behavior in the immiscible blend at temperatures below T_g . The absence of crystal growth at these temperatures allows for a detailed investigation of the nucleation behavior over time. This investigation provides new crucial information concerning the effects of chain mobility on nucleation behavior in the immiscible polymer blend.

Experimental Section

Materials. The PLLA (LACEA; $M_w = 1.3 \times 10^5$, $M_w/M_n = 1.49$) and PCL (Cellgreen; $M_w = 1.2 \times 10^4$, $M_w/M_n = 1.8$) samples were supplied by Mitsui Chemical Co. and Daicel Chemical Co., Japan, respectively. The polymers were purified by dissolving in chloroform, reprecipitated from heptane, and then dried in a vacuum oven at 40 °C for 24 h. Samples were then stored in a desiccator at room temperature until use.

Preparation of Blends. PLLA/PCL blend samples with various compositions were prepared by the solution casting method. Both polymers were dissolved in chloroform at total polymer content of 30 mg/mL and stirred at 40 °C for 5 h. The mixtures were then cast on Teflon dishes at 30 °C for 24 h. The obtained films were dried under vacuum for 24 h to remove residual solvent. The PCL content of the prepared blends was 1, 5, and 10 wt %, and named 9901, 9505, and 9010, respectively.

Differential Scanning Calorimetry (DSC). DSC thermograms of the samples (about 10 mg), which were presealed in aluminum pans, were recorded on a Pyris Diamond DSC (Perkin-Elmer). Dry nitrogen gas was let through the DSC cell at a flow rate at 20 mL/min. The temperature of the equipment was calibrated using the melting point of indium.

At first, samples were melted at 190 °C for 3 min and quenched to -20 °C at 50 °C/min. For the nonisothermal crystallization measurement, samples were heated from -20 to 200 at 20 °C/min. For the isothermal crystallization measurement, samples were rapidly heated at 500 °C/min to 140 °C and then isothermally crystallized. For the aging experiments, samples were heated to the desired temperatures, aged for 60, 120, or 240 min, and then heated to 140 at 500 °C/min and isothermally crystallized at that temperature.

Polarized Optical Microscopy (POM). The spherulite growth rate was determined during isothermal crystallization using an Olympus BX90 polarizing microscope (Olympus Co., Tokyo,

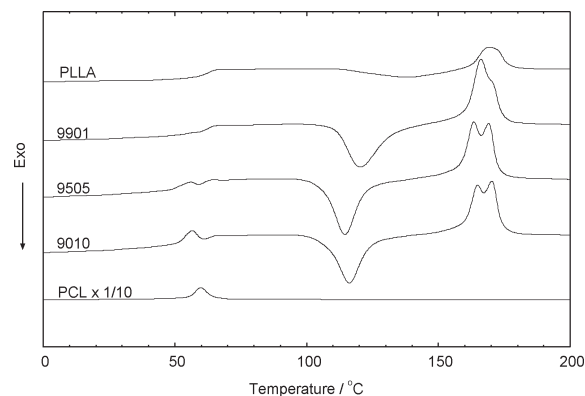


Figure 1. DSC heating scan of neat PLLA, neat PCL, and various blends. Samples were heated after holding at -20 °C for 3 min after being quenched from the melt. The rate of heating was 20 °C/min.

Japan) equipped with a digital camera system. The temperature was controlled by a Mettler FP82HT hot stage. The samples, which were prepared between microscope coverslips, were cooled to the desired temperature after melting at 190 °C for 3 min and isothermally crystallized. The diameter of more than five spherulites was measured for each sample during isothermal crystallization, and the growth rate was calculated by the least-squares method.

Results and Discussion

Miscibility and Crystallization Behavior. In order to ensure miscibility and the cold crystallization behavior of the PLLA/PCL blend system, we performed DSC nonisothermal heating scans of neat PLLA, PCL, and respective blends, and the thermograms are shown in Figure 1. T_g of the neat PLLA appeared at 60 °C, while T_g of 9901 appeared at 58 °C, which is slightly lower than that of neat PLLA. The steplike changes in heat capacity due to the glass transition could not be delineated since they overlapped with the melting peak of PCL. However, the change in heat capacities below and above the peak indicated that they were between 55 and 60 °C. T_g of a miscible polymer blend system is estimated by the Fox-Flory equation $1/T_g = \phi_1/T_g^1 + \phi_2/T_g^2$, where ϕ s represent the volume ratio of components with respective T_g corresponding to the suffixes.²¹ According to this equation, the expected T_g of 9901, 9505, and 9010 were calculated to be 58, 52, and 42 °C, respectively, using the T_g of PLLA = 60 °C and PCL = -60 °C (not shown in this figure). A PCL component of ca. 1–5 wt % in the blend seemed to allow for interactions with PLLA since T_g follows the Fox-Flory equation. For amounts greater than 5 wt %, T_g resulted in deviation from the equation. The modest decrease in T_g with the addition of PCL indicates the low miscibility of this system. This result is consistent with that observed by others.¹⁰

The cold crystallization behavior of PLLA was also influenced by the presence of PCL. While neat PLLA showed a broad exothermic peak around 125 °C, peaks of the blends appeared sharper and their position decreased with increasing PCL content, reaching 105 °C with 10 wt % of PCL. This indicates that PCL enhanced the crystallization of PLLA at low temperature. Crystallization consists of mainly two processes, comprising nucleation of the crystal and crystal growth. In the PLLA/PCL blend, since the enhancement effect of PLLA crystallization is seen even with low PCL content, PCL seems to accelerate not the crystal growth of PLLA, but mainly the generation of nuclei.

Spherulite Growth Rate by POM. In an effort to investigate the manner by which PCL affects the cold crystallization, we measured the growth rate of spherulites of neat PLLA and blends using POM, and the results are shown in

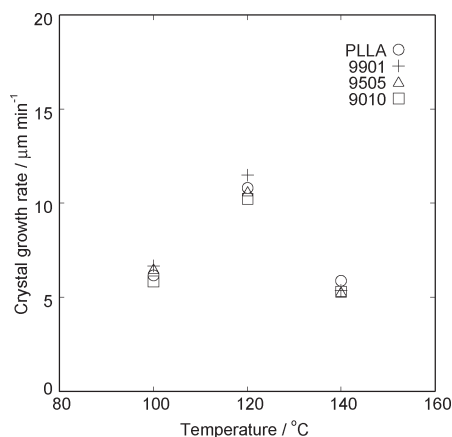


Figure 2. Spherulite growth rate of neat PLLA and blends at temperatures from 100 to 140 °C.

Figure 2. The growth rates below 100 °C were unmeasurable given the vast abundance of nuclei at lower crystallization temperatures which obscured the identification of spherulites. The growth rate of PLLA showed a maximum at around 120 °C, and all the blends showed similar values to neat PLLA at each temperature regardless of the PCL content, indicating that PCL has an insignificant effect on the crystal growth of PLLA, perhaps due to the low miscibility of PCL in the blend. As might be expected, the PCL chains inside of the domains are unable to interact with PLLA chains, and this affects the growth rate of the bulk PLLA. Consequently, the enhancement effect of cold crystallization is certainly the result of the increase in the number of nuclei generated at lower temperature induced by the presence of PCL.

Isothermal Crystallization Measurements after the Aging Process. Since the enhancement of cold crystallization in the PLLA/PCL blend was confirmed to reflect the acceleration of nucleation of PLLA, we then investigated the nucleation behavior during aging below T_g . The increase in the nuclei density was observed to follow the enhancement of cold crystallization. The cold crystallization behavior of the blends and neat PLLA could be used for a comparison of nuclei density without any correction since the crystal growth rate of PLLA was independent of the PCL content. However, the use of DSC nonisothermal heating scans to determine the nuclei density generated in the aging process is unsuitable since many nuclei will be generated during the scanning process, especially just above T_g . Thus, in order to investigate nucleation occurring in the aging process, we performed isothermal crystallization measurements of DSC at 140 °C, where the rate of self-nucleation is negligibly small, following aging at temperatures below T_g . Figure 3a shows the temperature sequence of the isothermal crystallization measurement. Samples were aged at 0 °C for 60, 120, and 240 min after being quenched from melt, then rapidly heated to 140 at 500 °C/min, and isothermally crystallized. This process minimizes nucleation during heating since samples rapidly cross the temperature range just above T_g where nucleation easily occurs.

Figure 3b shows the result of isothermal crystallization for neat PLLA and the blends aged at 0 °C for various aging periods. The apparent exothermic peaks are due to the heat of crystallization. Neat PLLA showed little change in crystallization behavior with aging time, indicating that few nuclei were generated during the aging process. The low chain mobility below the glass transition seemed to restrict the generation of nuclei. Although it was reported that nuclei

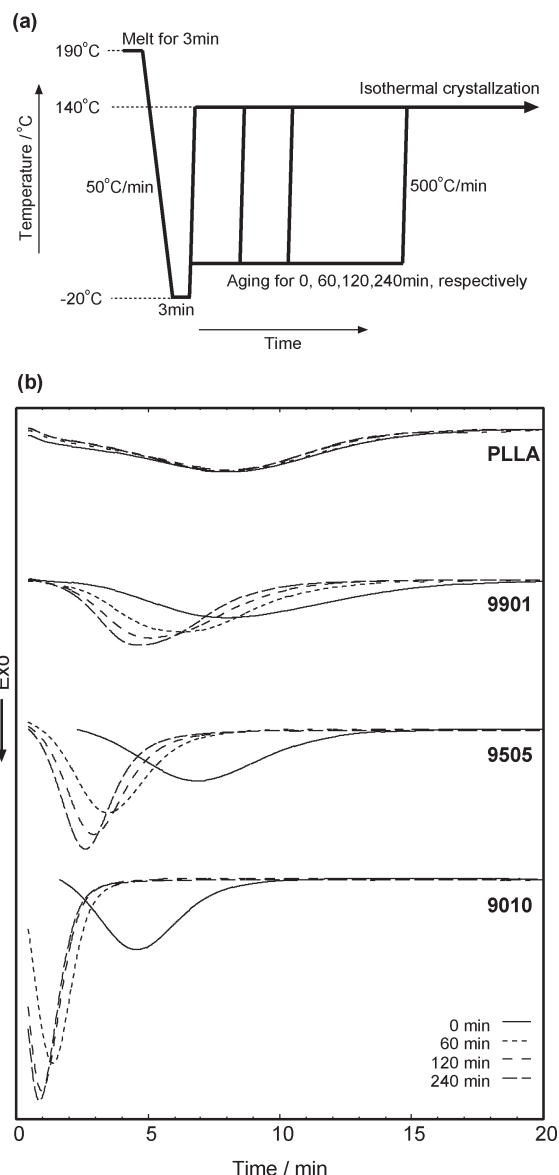


Figure 3. DSC isothermal crystallization measurements after the aging process at 0 °C. (a) Thermal processing of the measurement. Samples were first melted at 190 °C for 3 min, then quenched to -20 at 50 °C/min, and held for 3 min. They were rapidly heated to 0 at 500 °C/min and aged for given periods and then rapidly heated to 140 at 500 °C/min. (b) The heat flow curve of the isothermal crystallization of neat PLLA and blends after aging at 0 °C for 0, 60, 120, and 240 min.

were generated even below T_g ,^{19,20} the rate was quite slow and occurred in the space of dozens of hours. Therefore, the change in our case can be negligible due to the relative shorter aging time. On the contrary, crystallization of the blends was markedly enhanced with aging time. This indicates that nucleation took place even below T_g .

In an effort to estimate the increase in nuclei density during the aging, we performed Avrami analysis.²² The isothermal heat flow curve was integrated to determine the relative crystallinity X_t as a function of time. The relative crystallinity X_t at any given time was calculated from the integrated area of the DSC curve from $t = 0$ to t divided by the integrated area of the whole heat flow curve. The isothermal crystallization kinetics were analyzed with the Avrami equation

$$X_t = 1 - \exp(-kt^n) \quad (1)$$

Table 1. Parameters of Avrami Analysis for the Neat PLLA and the Blends with Various Aging Time^a

sample	aging time [min]	<i>n</i> unfixed			<i>n</i> fixed to 3.0		
		<i>n</i>	log <i>k</i>	<i>t</i> _{1/2}	log <i>k</i>	<i>k</i> [min ⁻³]	<i>k</i> - <i>k</i> _{PLLA} [min ⁻³]
PLLA 0 °C	0	2.65	-2.61	8.12	-2.99	0.001 02	0
	60	2.50	-2.47	8.07	-2.97	0.001 07	0
	120	2.72	-2.64	8.08	-2.88	0.001 31	0
	240	2.76	-2.64	7.92	-2.86	0.001 38	0
9901 0 °C	0	2.94	-3.00	8.12	-3.05	0.000 89	b
	60	2.92	-2.58	8.30	-2.64	0.002 29	0.001 22
	120	2.88	-2.39	7.98	-2.48	0.003 31	0.002 00
	240	2.95	-2.32	7.60	-2.36	0.004 36	0.002 98
9505 0 °C	0	3.48	-3.14	6.85	-2.70	0.001 99	0.000 97
	60	3.20	-2.02	3.45	-1.88	0.013 1	0.011 8
	120	2.97	-1.68	2.93	-1.69	0.020 4	0.019 1
	240	2.91	-1.50	2.62	-1.54	0.028 8	0.027 4
9010 0 °C	0	3.41	-2.49	4.53	-2.18	0.006 60	0.006 50
	60	2.78	-0.68	1.38	-0.71	0.194	0.193
	120	2.56	-0.38	0.95	-0.41	0.389	0.388
	240	2.51	-0.34	0.90	-0.36	0.436	0.435

^a *n* and log *k* in the center column were estimated by two-parameter fitting (*k* and *n*), and log *k* and *k* in the right column were estimated by fitting with *n* fixed to 3. *k* - *k*_{PLLA} is the value of respective *k* subtracted by the *k* of the neat PLLA of corresponding period of aging. ^b The value is almost zero although the calculation result is minus.

where *n* is the Avrami index, which relates to the dimensional growth and way in which primary nuclei are formed, and *k* is the whole crystallization rate constant associated with both nucleation and growth contributions. The linear form of eq 1 is given as eq 2:

$$\log[-\ln(1 - X_t)] = \log k + n \log t \quad (2)$$

The results are summarized in Table 1, where the Avrami index *n* was obtained by plotting log[-ln(1 - *X_t*)] against log *t* with the linear least-squares method (see the Supporting Information), and the resulting values of all samples were between 2.5 and 3.5. This index represents the dimension of crystal growth. In the case of a homogeneous nucleation system, when nuclei are generated gradually during the crystallization, the growth dimension is (*n* - 1). On the other hand, in the case of a homogeneous nucleation system, when the nuclei are generated after the onset of the crystallization, the growth dimension is *n*. In our case, the dimension of growth should be ~3 since spherulites were observed by POM, and subsequently obtained indexes *n* = 2.5–3.5 indicate that crystallization of PLLA followed that of a heterogeneous nucleation system. The density of nuclei should increase linearly during crystallization in homogeneous nucleation, while it remains constant in heterogeneous nucleation.²³ Therefore, we can consider that generation of nuclei during isothermal crystallization is negligible compared to the initial density of nuclei generated during the aging process.

It is well-known that Avrami analysis is unable to follow the experimental crystallization completely for several reasons which include secondary crystallization and the slight crystallization present prior to the beginning of measurements, thereby resulting in errors in *n* values. Thus, we performed the Avrami analysis with index *n* fixed to 3.0 in an effort to compare the whole crystallization rate *k* between various samples. The fitted results, log *k*_(*n* = 3), are shown in the right column of Table 1 (see the Supporting Information). The relation between the whole crystallization rate *k* and density of nuclei *I* in the case of *n* = 3 is represented by following equation:

$$k = \frac{4}{3} I \pi G^3 \quad (3)$$

The equation reflects the proportional relation between *k* and *I*, indicating the value *k* enable to be regarded as relative

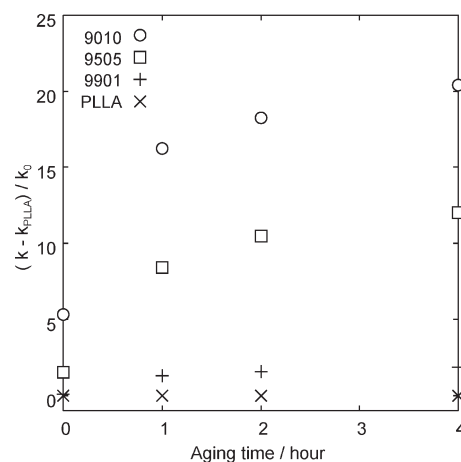


Figure 4. Change in relative nuclei density *k* - *k*_{PLLA} of neat PLLA as well as 9901, 9505, and 9010 with aging time. *k* - *k*_{PLLA}s were divided from *k*₀ which represents the *k* value of nonaged neat PLLA to normalize.

nuclei density. In the following discussion, we mainly use relative nuclei density *k* to show the change in nuclei density.

As shown in Table 1, neat PLLA showed little change in *k* value with aging time, which is consistent with the heat flow curve shown in Figure 3. This indicates that few nuclei were generated during the aging process in neat PLLA. In contrast, the cold crystallization behavior of the blends was dependent on the aging time over several hours; the longer the sample was aged, the larger *k* value was obtained. This indicates the nuclei were generated during the aging process in the blend system. Even though the *T_g* of PLLA was depressed slightly by the presence of PCL, the change is quite small as shown with the DSC heating scan. Therefore, the average mobility of the PLLA chains is insufficient to generate nuclei at the aging temperature, which is sufficiently lower than the *T_g* of PLLA. This suggests that another immiscible component plays an important role in the nucleation.

We calculated *k* - *k*_{PLLA} values to represent the nuclei density induced only by PCL, where *k*_{PLLA} is the *k* value of neat PLLA with respective aging time. *k* - *k*_{PLLA} values of aged samples of each blend are shown in Table 1. We plotted (*k* - *k*_{PLLA})/*k*₀ against the aging time in Figure 4 to show the change in nuclei density with aging time. The denominator *k*₀

Table 2. Parameters of Avrami Analysis for the Neat PLLA and 9901 with Various Aging Temperature

sample	aging time [min]	<i>n</i> unfixed			<i>n</i> fixed to 3.0		
		<i>n</i>	log <i>k</i>	<i>t</i> _{1/2}	log <i>k</i>	<i>k</i> [min ^{−3}]	<i>k</i> − <i>k</i> _{PLLA} [min ^{−3}]
PLLA 40 °C	0	2.63	−2.61	8.12	−2.99	0.001 02	0
	60	2.94	−2.86	8.30	−2.92	0.001 20	0
	120	3.02	−2.89	7.98	−2.87	0.001 34	0
	240	3.08	−2.89	7.60	−2.81	0.001 54	0
9901 0 °C	0	2.94	−3.00	8.07	−3.05	0.000 89	^a
	60	2.92	−2.58	6.28	−2.64	0.002 29	0.001 09
	120	2.88	−2.39	5.10	−2.48	0.003 31	0.001 97
	240	2.95	−2.32	4.63	−2.36	0.004 36	0.002 82
9901 20 °C	0	2.94	−3.00	8.07	−3.05	0.000 89	^a
	60	3.42	−2.82	5.65	−2.47	0.003 38	0.002 18
	120	3.22	−2.49	5.15	−2.31	0.004 89	0.003 55
	240	3.42	−2.53	4.60	−2.20	0.006 30	0.004 76
9901 25 °C	0	2.94	−3.00	8.07	−3.05	0.000 89	^a
	60	3.24	−2.47	4.70	−2.28	0.005 24	0.004 04
	120	3.23	−2.32	4.23	−2.14	0.007 24	0.005 90
	240	3.37	−2.24	3.77	−1.98	0.010 4	0.008 86
9901 30 °C	0	2.94	−3.00	8.07	−3.05	0.000 89	^a
	60	3.07	−2.03	3.76	−1.98	0.010 4	0.009 20
	120	3.27	−2.08	3.40	−1.91	0.012 3	0.011 0
	240	3.11	−1.85	3.03	−1.79	0.016 2	0.014 7
9901 35 °C	0	2.94	−3.00	8.07	−3.05	0.000 89	^a
	60	3.28	−1.88	2.90	−1.73	0.018 6	0.017 4
	120	3.07	−1.67	2.60	−1.63	0.023 4	0.022 1
	240	3.55	−1.72	2.38	−1.47	0.033 8	0.032 3
9901 40 °C	0	2.94	−3.00	8.07	−3.05	0.000 89	^a
	60	2.61	−1.32	2.15	−1.55	0.028 1	0.026 9
	120	2.88	−1.28	1.98	−1.35	0.044 6	0.043 2
	240	2.85	−1.15	1.75	−1.24	0.057 5	0.056 0
9901 45 °C	0	2.94	−3.00	8.07	−3.05	0.000 89	^a
	60	2.57	−1.01	1.58	−1.19	0.064 5	0.063 3
	120	2.61	−0.86	1.30	−0.99	0.102	0.101
	240	2.59	−0.73	1.13	−0.86	0.138	0.136

^aThe value is almost zero although the calculation result is minus.

is the *k* of nonaged neat PLLA to normalize *k* − *k*_{PLLA}. It is noteworthy that (*k* − *k*_{PLLA})/*k*₀ of each blend exhibited saturation behavior with aging time, and the asymptotic values increased with PCL content. This saturation behavior indicates that the number of sites where nucleation could occur is limited. We can regard this nucleation behavior as following heterogeneous nucleation, which means that nuclei can be generated only at particular sites, denoted by active sites.²³ The asymptotic value of the nuclei density represents the number of active sites. Although number of PCL domains is not accurately proportionate to the content of PCL since it depends on both the PCL content and the domain size, the number should increase at least in low content range of PCL. Thus, the increase in the asymptotic value with PCL content indicates that the nucleation of PLLA is enhanced at PCL domains, which heterogeneously disperse in the PLLA matrix. It follows from these results that PCL domains acted as active sites for the nucleation of PLLA.

In an effort to examine the acceleration mechanism of the nucleation, we shall refer to the classic theory of nucleation kinetics. Nucleation is an activation process and its rate *R* can be represented by the following equation:²³

$$R = A \exp \left[-\frac{\Delta G_S + \Delta G_D}{kT} \right] \quad (4)$$

where ΔG_S is the activation barrier of the surface free energy to form the crystal nuclei and ΔG_D is the barrier related to chain mobility. *A* is assumed to be constant for the given experimental temperature range. ΔG_S is represented by $\Delta G_S \propto \sigma^3 V_m^2 / 3 \Delta G^2$, where ΔG is the bulk free energy change in the liquid to crystal transformation (per mole) and V_m is the molar volume of the crystal phase. Since ΔG depends on

the extent of supercooling from the equilibrium melting temperature, ΔG_S decreases as the temperature decreases. On the other hand, ΔG_D can be expressed in terms of an effective diffusion coefficient in the liquid given by $D = D_0 \exp(-\Delta G_D/kT)$, where D_0 is constant at experimentally narrow temperature ranges. The diffusion coefficient *D* decreases markedly at *T*_g due to restrictions in chain mobility, which follows that ΔG_D will increase sharply below *T*_g. Therefore, the nucleation rate *R* exhibits a maximum just above *T*_g and rapidly decreases below *T*_g.²⁴ The negligible nucleation of neat PLLA during aging below *T*_g, as reported by other authors,^{19,20} seems to be due to an increase in ΔG_D .

Consequently, two reasons could be employed to account for the acceleration of nucleation, being a decrease in ΔG_S resulting from a decrease in the surface free energy and a decrease in ΔG_D resulting from activation of chain mobility. The presence of a phase interface with the PCL domain, regardless of whether it is amorphous or crystalline, could be considered to reduce barrier of the surface free energy ΔG_S .^{12,13} However, since the term ΔG_D dominates the nucleation rate at temperatures below *T*_g, the decrease in ΔG_S seemed no longer to affect the nucleation rate. Thus, it is supposed that ΔG_D , namely chain mobility, takes on a primary role in the nucleation.

Temperature Dependence of the Nucleation Effect. The nucleation mechanism is strongly dependent on the temperature as mentioned above. Therefore, an investigation of the dependence of aging temperature on nucleation would help to delineate the mechanism involved. Isothermal crystallization measurements were performed with samples subjected to various aging temperatures. Unfortunately, the blends with high PCL content crystallized so rapidly that an Avrami analysis could not be conducted. Thus, the temperature dependence analysis was conducted only for

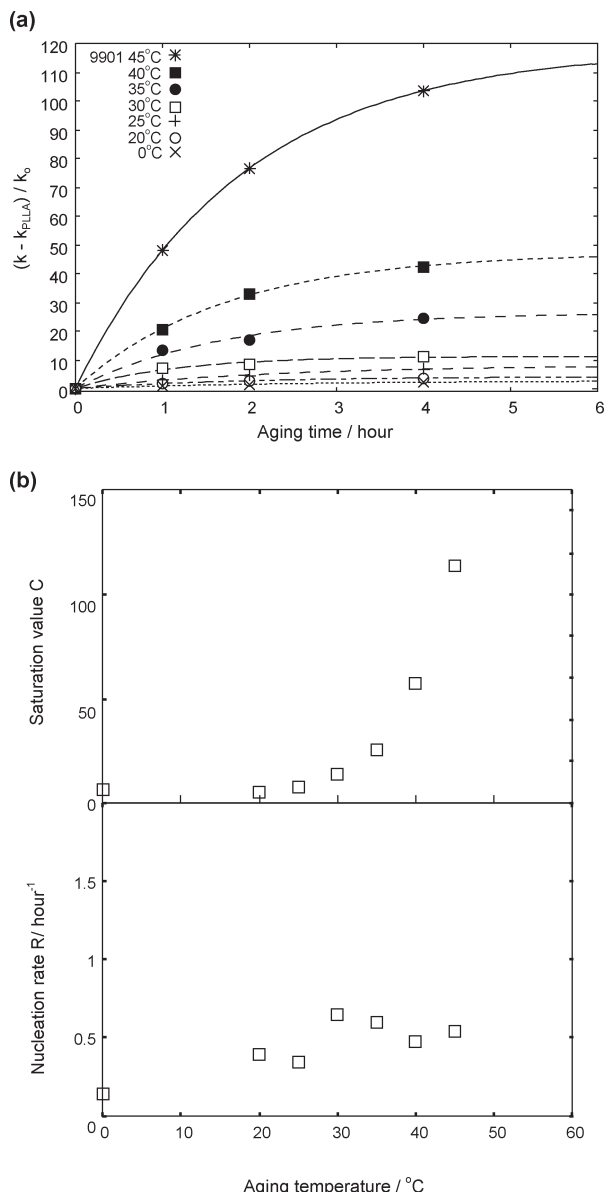


Figure 5. Change in nuclei density of neat PLLA and 9901 for various aging temperatures. (a) Relative nuclei density $(k - k_{\text{PLLA}})/k_0$ with aging time. The lines are the result of fitting of the first-order reaction equation: $(k - k_{\text{PLLA}})/k_0 = C(1 - \exp(-Rt))$. (b) Fitted parameters C and R , which represent the density of the active site and nucleation rate, respectively, at various aging temperatures.

the blend comprising a PCL content of 1 wt %. The isothermal crystallization at 140 °C was measured for 9901 after aging at various temperatures and periods.

Results of the Avrami analysis are summarized in Table 2, and $(k - k_{\text{PLLA}})/k_0$ was plotted against aging time in Figure 5a (see the Supporting Information). The density of nuclei showed saturation behavior with aging time at all aging temperatures. In an effort to estimate the nucleation rate at each temperature, we approximated the plots using the following equation of a first-order reaction

$$(k - k_{\text{PLLA}})/k_0 = C(1 - \exp[-Rt]) \quad (5)$$

where coefficient C represents a finite number of nuclei and R is the increase in rate of nuclei. This equation assumes that nucleation occurs at active sites with density of C at a uniform rate of R . The lines in Figure 5a are fitted curves

of each plot. All plots were well fitted by the equation, indicating that the nucleation could be regarded as heterogeneous nucleation. We plotted C and R as functions of the aging temperature as shown in Figure 5b. The value of R remained almost constant at all aging temperatures, while the density of the active site C decreased as the temperature decreased, reaching almost zero at around 20 °C.

Before looking at the nucleation rate, we should make mention of the temperature dependence of C . It is noteworthy that the active site density C decreased as the aging temperature decreased. The dispersion states of PCL should be identical among all samples since they were quenched in the same way. Therefore, this result suggests that the presence of PCL domains do not always lead to the nucleation of PLLA. The lower temperature, more PCL domains lose the ability to facilitate nucleation, meaning that the ability to activate nucleation of PLLA seems to be nonuniform among the PCL domains.

We shall return to the nucleation rate R . Interestingly, the obtained nucleation rate changed negligibly with aging temperature. The nucleation temperature range of the measurements was below T_g , at around 60 °C, and as an indication, the Vogel temperature of neat PLLA has been reported to be 24 °C.²⁵ Thus, if the chain mobility of neat PLLA was the only factor taken into consideration, the nucleation rate should decrease markedly as the temperature decreases due to the glass transition. However, no significant change with aging temperature was observed in R , indicating that the presence of PCL lead to deviation of R from the expected temperature dependence. The result indicates that at the active site the marked decrease in ΔG_D is locally evaded. This indicates that the presence of PCL ensures chain mobility of PLLA, thereby resulting in nucleation of PLLA at the interface of its domains.

The interaction with PCL, which has a lower T_g than PLLA, is possible to allow for activation of chain mobility of PLLA. In other words, T_g of PLLA could be lowered by interaction with PCL, resulting in declination of the glass transition of PLLA. However, the blend with PCL content of 1 wt % exhibited nucleation even at 20 °C, which is as much as 40 °C lower than T_g of PLLA, while the T_g obtained by DSC showed a subtle change. This discrepancy can be accounted for if we consider the limited miscibility of the PLLA/PCL blend and the consequent aggregation of PCL to be important. If PLLA and PCL were miscible, the added PCL would disperse homogeneously into the matrix PLLA, thus facilitating a decrease in T_g . However, in this case, the extent of the decrease in T_g is small when the PCL content is low. On the other hand, a phase-separated component in a completely immiscible system is unable to affect T_g of the opposite component. However, even in the case of immiscible blend systems, molecular chain interpenetration occurs at the phase interface depending on the Flory–Huggins χ parameter,^{26–31} and the components mutually affect chain mobility at the phase interface.^{32,33} Although the χ parameter of the PLLA/PCL blend has not been reported, several reports have claimed some degree of compatibility between PLLA and PCL.^{10,34} Therefore, we speculate that aggregated PCL could facilitate a local and deep depression of T_g , thereby resulting in nucleation at the interface of the domains.

Although depression of T_g at the active site could ensure chain mobility, the mobility should depend on the distance of the aging temperature from the locally depressed T_g . Therefore, we need to determine whether this speculation is consistent with the temperature independence of the nucleation rate R . Before this issue is discussed, a comment should be

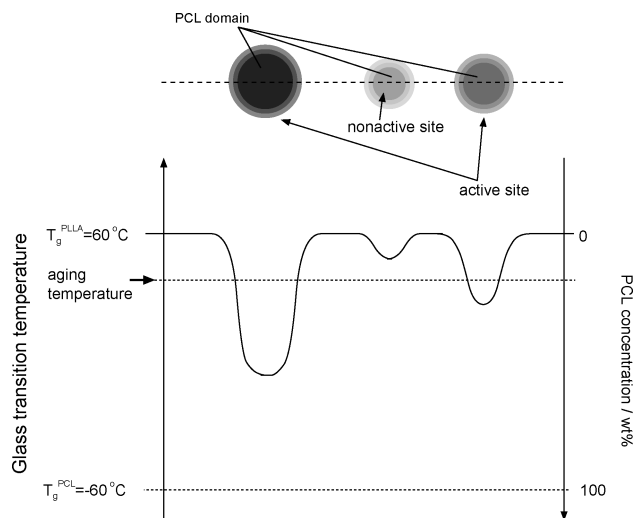


Figure 6. A model of the depression of T_g induced by PCL domains. The upper figure represents aggregated PCL domains in the PLLA matrix, and shadings correspond to the concentration of PCL. The bottom graph shows the T_g of PLLA and PCL concentration along the dotted line in the upper figure. Domains with T_g lower than the aging temperature could ensure PLLA chain mobility at the interface and act as active sites.

made concerning the behavior of the C value. The temperature dependence of experimentally obtained C reflects differences in the nucleation ability among the domains. This can be explained by the distribution of depth of the depressed T_g . A proposed model is shown in Figure 6. In this model, we assume that PCL domains contain to some extent PLLA due to its limited miscibility, and each domain has T_g corresponding to the PCL concentration. Around a PCL domain which has T_g lower than the aging temperature, T_g of PLLA falls below the aging temperature at the interface, thereby resulting in nucleation. This model implies that only PCL domains which have T_g lower than the aging temperature could act as active sites for PLLA nucleation. Thus, the lower the temperature, the fewer active sites are present, which is consistent with the experimental behavior of C . The T_g distribution seems to be realized by the distribution of PCL concentration among all the PCL domains. Disappearance of the active site below ca. 20 °C implies that T_g of PLLA locally depressed at the interface of PCL domains is at least higher than 20 °C. This suggests that almost all of the PCL domains have relatively high PLLA content in the blend with a PCL content of 1 wt %.

The temperature independence of the nucleation rate R could be accounted for by the following two reasons. First, the temperature dependence of chain mobility above T_g is not very significant. Thus, the slope of the nucleation rate should be gentle given the presence of a local maximum in the nucleation rate just above T_g . Besides, as shown in Figure 5a, the number of active sites decreased precipitously as the temperature decreased. This indicates that the active sites which have greatly depressed T_g , such as domains with T_g at 20 °C, occupy only a small proportion relative to the total number of PCL domains. Therefore, the active sites which have a high nucleation rate have limited effect on R , which represents the averaged nucleation rate of all the active sites.

The indication that sufficient chain mobility is required for the nucleation is consistent with the result by other authors. Han et al. revealed that nucleation is enhanced by the concentration fluctuation due to the spinodal decomposition of LLPS.^{15,16} They speculated that the dynamic effect of

concentration fluctuation induces the specific chain alignment at the phase interface and subsequent nucleation. Although our case of PLLA/PCL blend system does not accompany the spinodal decomposition, the deep quench from melt state to the temperature below T_g might generate a new equilibrium state. It can be a thermodynamic driving force for the diffusion flux of polymer chains at the surface of the PCL domain. Considering the T_g of the PLLA observed by DSC measurement changed little by addition of 1 wt % of PCL, chain mobility of PLLA is seemingly restricted at the given temperatures in our experiment. However, if there is sufficient chain mobility locally activated by PCL, the dynamic chain alignment could take place. At the same time, with sufficient mobility, PLLA can even nucleate by itself due to the energetic favorability. The nucleation also might be enhanced by the presence of the surface of crystalline or amorphous PCL.^{12,13} At this time, unfortunately, we cannot determine which effect, that is the dynamic chain alignment or the static energetic effect, is dominant. Therefore, in order to delineate the mechanism of nucleation, additional observations of the interface with high space resolution such as electromicroscopies are required.

In any case, the nucleation behavior below T_g suggests that the activation of chain mobility takes on a significant role in nucleation enhancement in immiscible blend systems. Moreover, the aggregation of PCL due to the limited miscibility of PLLA/PCL seems to facilitate the local and deep depression of T_g at the interface. Our speculated model presents an important suggestion for the nucleation mechanism: the nucleation at the phase interface of immiscible blends is not dominated by average T_g , but locally modified T_g due to the interchain interaction. The present quantitative analysis revealed that the nucleation rate is independent of the aging temperature.

Conclusion

We revealed that the nucleation of PLLA occurred during aging even at temperature below T_g of PLLA in the PLLA/PCL blend system. Since the increase in nuclei density of PLLA showed saturation behavior with aging time, the nucleation is supposed to follow that of a heterogeneous nucleation system in which PCL domains act as active sites. The nucleation rate R was almost independent of the aging temperature in the blend with PCL content of 1 wt %, although it was expected to decrease with the glass transition due to a lowering of chain mobility. This suggests that the presence of PCL activates PLLA chain mobility. Nucleation was observed even at 20 °C, as much as 40 °C lower than T_g , following the addition of only 1 wt % PCL, while the T_g obtained by the DSC measurement showed a subtle decrease. This suggests that the limited miscibility of PLLA/PCL leads to the aggregation of PCL and depresses T_g locally and deeply at the interface of PCL domains, resulting in strong enhancement of PLLA nucleation.

Supporting Information Available: Plots of $\log[-\ln(1 - X_t)]$ against $\log t$ with the result of Avrami fitting. This material is available free of charge via the Internet at <http://pubs.acs.org>.

References and Notes

- (1) Leclair, A.; Favis, B. D. *Polymer* **1996**, *37*, 4723.
- (2) Horiuchi, S.; Matchariyakul, N.; Yase, K.; Kitano, T.; Choi, H. K.; Lee, Y. M. *Polymer* **1997**, *38*, 59.
- (3) Oslanec, R.; Brown, H. R. *Macromolecules* **2003**, *36*, 5839.
- (4) Boucher, E.; Folkers, J. P.; Creton, C.; Hervet, H.; Leger, L. *Macromolecules* **1997**, *30*, 2102.
- (5) Ikada, Y.; Tsuji, H. *Macromol. Rapid Commun.* **2000**, *21*, 117.
- (6) Tsuji, H.; Horikawa, G. *Polym. Int.* **2007**, *56*, 258.

- (7) Maglio, G.; Migliozi, A.; Palumbo, R.; Immirzi, B.; Volpe, M. G. *Macromol. Rapid Commun.* **1999**, *20*, 236.
- (8) Chen, C.; Chueh, J.; Tseng, H.; Huang, H.; Lee, S. *Biomaterials* **2003**, *24*, 1167.
- (9) Wu, D.; Zhang, Y.; Zhang, M.; Zhou, W. *Eur. Polym. J.* **2008**, *44*, 2171.
- (10) López-Rodríguez, N.; López-Arraiza, A.; Meaurio, E.; Sarasua, J. R. *Polym. Eng. Sci.* **2006**, *46*, 1299.
- (11) Dell'Erba, R.; Groeninckx, G.; Maglio, G.; Malinconico, M.; Migliozi, A. *Polymer* **2001**, *42*, 7831.
- (12) Bartczak, Z.; Galeski, A.; Krasnikova, N. P. *Polymer* **1987**, *28*, 1627.
- (13) Wenig, W.; Asresahegn, M. *Polym. Eng. Sci.* **1993**, *33*, 877.
- (14) Tsuburaya, M.; Saito, H. *Polymer* **2004**, *45*, 1027.
- (15) Zhang, X.-H.; Wang, Z.-G.; Dong, X.; Wang, D.-J.; Han, C. C. *J. Chem. Phys.* **2006**, *125*, 024907.
- (16) Zhang, X.-H.; Wang, Z.-G.; Muthukumar, M.; Han, C. C. *Macromol. Rapid Commun.* **2005**, *26*, 1285.
- (17) Wang, H.; Shimizu, K.; Hobbie, E. K.; Wang, Z.; Meredith, J. C.; Karim, A.; Amis, E. J.; Hsiao, B. S.; Hsieh, E. T.; Han, C. C. *Macromolecules* **2002**, *35*, 1072.
- (18) Ma, Y.; Zha, L.-Y.; Hu, W.-B.; Reiter, G.; Han, C. C. *Phys. Rev. E: Stat. Phys., Plasmas, Fluids* **2008**, *77*, 06180.
- (19) Pan, P.; Zhu, B.; Inoue, Y. *Macromolecules* **2007**, *40*, 9664.
- (20) Sánchez, F. H.; Mateo, J. M.; Colomer, F. J. R.; Sánchez, M. S.; Ribelles, J. L. G.; Mano, J. F. *Biomacromolecules* **2005**, *6*, 3238.
- (21) Fox, T. G.; Flory, P. J. *J. Appl. Phys.* **1950**, *21*, 581.
- (22) Avrami, M. *J. Chem. Phys.* **1940**, *8*, 212.
- (23) James, P. F. *Adv. Ceram.* **1982**, *4*, 1.
- (24) Gonzalez-Oliver, C. J. R.; James, P. F. *J. Non-Cryst. Solids* **1980**, *38*, 699.
- (25) Murakami, H.; Araki, O.; Masuda, T. *J. Soc. Rheol. Jpn.* **2000**, *28*, 193.
- (26) Flory, P. J. *J. Chem. Phys.* **1953**, *10*, 51.
- (27) Helfand, E.; Tagami, Y. *J. Chem. Phys.* **1972**, *56*, 3592.
- (28) Helfand, E. *J. Chem. Phys.* **1972**, *57*, 1812.
- (29) Rigby, D. *Macromolecules* **1985**, *18*, 2269.
- (30) Tan, S. S.; Zhang, D. H.; Zhou, E. L. *Polymer* **1997**, *38*, 4571.
- (31) Farinha, J. P. S.; Vorobyova, O.; Winnik, M. A. *Macromolecules* **2000**, *33*, 5863.
- (32) Cameron, G. G.; Buscall, D. S. *Polymer* **1996**, *37*, 5329.
- (33) Cameron, G. G.; Qureshi, M. Y.; Buscall, D. S.; Nemcek, J. *Polymer* **1995**, *36*, 3071.
- (34) Newman, D.; Laredo, E.; Bello, A.; Grillo, A.; Feijoo, J. L.; Muller, A. J. *Macromolecules* **2009**, *42*, 5219.